JOURNAL OF SOLID STATE CHEMISTRY **129,** 123–129 (1997)
ARTICLE NO. SC967249

Crystal and Magnetic Structures of a Nickel-Rich Ferrite Obtained by Ionic Exchange from α-$NaFeO_2$

M. C. Blesa,* E. Morán,* U. Amador,[†,‡,1] and N. H. Andersen[§]

*Departamento de Química Inorgánica, and [†]C.A.I. Difracción de Rayos-X, Facultad de Ciencias Químicas, Universidad Complutense, 28040 Madrid, Spain; [‡]Facultad de Ciencias Experimentales y Técnicas, Universidad San Pablo-C.E.U., Urb. Montepríncipe, Apdo. Correo 67, E-28668, Boadilla del Monte, Madrid, Spain; and [§]Department of Solid State Physics, Risø National Laboratory, DK-4000 Roskilde, Denmark

Received July 5, 1996; accepted November 27, 1996

The crystallographic structure of a hyperstoichiometric $Ni_{1+x}Fe_{2-2x/3}O_4$ ($x=0.30$) spinel-like material, obtained by a soft chemistry synthetic route, has been refined by combining X-ray and neutron powder diffraction data. This compound shows a structure intermediate between the rocksalt and the spinel structure types. The results of the refinement of the magnetic structure are also presented and discussed.

INTRODUCTION

Ferrites are ceramic oxidic materials widely used in many technological applications, most of them based on their magnetic properties (1). Particularly, the nickel ferrite $NiFe_2O_4$, whose structure is spinel-like, exists in a certain composition range and shows interesting properties, many of them related to magnetic aftereffects (2–4). Besides, it exhibits, useful chemical properties as a catalyst for the commercial production of phenol (5) or the decomposition CO_2 to carbon (6). Although this ferrite has been known for decades (7) there is at present a renewed interest in it, specially due to some magnetic properties such as disaccommodation, ferromagnetic relaxation and ferromagnetic resonance which are prominent in this material (8, 9). Both the magnetic and the catalytic properties are dependent on the particular structural features, on the particle size and on the preparation conditions as well.

Nickel ferrites are usually obtained by the ceramic method from stoichiometric mixtures of the corresponding oxides NiO and Fe_2O_3 at temperatures between 1100 and 1600°C (10, 11), though other alternatives are also being explored, for instance the synthesis of this material in nanocrystalline form has been recently achieved by means of a special synthetic procedure (12). In our case the title material was obtained by an ionic exchange reaction at 500°C. In this connection it is worth to note that cation exchange reactions in molten salts may be used on a variety of metal oxides to form new phases. Whenever these reactions are performed at sufficiently low temperature, extensive parts of the original framework are retained and only minor structural rearrangements take place (13); thus, under these conditions the reaction can be considered as topotactic.

In a previous paper (14) we reported the exchange reaction of α-$NaFeO_2$ in molten nitrates with divalent cations (Ni and Mg), the ferrites so obtained being studied by X-ray diffraction, Mössbauer spectroscopy, and magnetization measurements. As it is well known, X-ray diffraction cannot distinguish between Fe and Ni; thus, the cation distribution proposed was obtained taken into account the results from spectroscopic techniques and magnetic measurements. Worthy of note is that the structure of the nickel ferrite obtained by these means differs from the simple spinel-like because some extra positions, usually empty in the spinel structure, are partially occupied. In this connection, some authors have recently remarked the close relationships existing between the spinel and the rock-salt structures, either based on crystallochemical considerations (15) or on the "*in situ*" observation of the phase transition spinel ⇒ rock-salt induced by the electron beam of an electron microscope (16).

We report in this paper the results of neutron powder diffraction experiments performed to elucidate the complex cation distribution of this material. The magnetic structure has also been refined.

EXPERIMENTAL

Synthesis

The precursor α-$NaFeO_2$ was prepared by reaction between α-Fe_2O_3 and Na_2O_2 in air at 500°C, following the procedure described by Takeda (17).

The nickel ferrite was obtained from α-$NaFeO_2$ by ionic exchange in molten salts: 10 g of the precursor and 35 g of

[1] To whom correspondence should be addressed

0022-4596/97 $25.00

an eutectic mixture of potassium and nickel chlorides (molar composition 80.3% KCl and 19.7% $NiCl_2$, with a melting point of 494°C) were kept at 500°C for 24 hr.

The reaction can be schematized as follows:

$$2\alpha\text{-}NaFeO_2 + (1 + x)NiCl_2 \rightarrow Ni_{1+x}Fe_{2-2x/3}O_4 + 2NaCl + 2x/3\,FeCl_3. \quad [1]$$

An excess of nickel chloride has been used in order to obtain hyperstoichiometric samples with regards to the ideal composition $NiFe_2O_4$. The final product was washed with hot water to remove the excess of chlorides.

Characterization

The materials prepared by the above describe methods were confirmed to be essentially single phase samples by X-ray diffraction (XRD) on a Siemens D-5000 apparatus using a monochromatic Cu(K_α) beam and operated in the step scan technique, with a step size of 0.02° and a step time of 15 s/step. When a very long counting time is used, i.e., 90 s/step, a number of quite small peaks corresponding to an unidentified impurity phase appear. These impurity phase is also observed in the neutron diffraction pattern obtained with neutrons of a long wavelegth.

Chemical analysis was performed by Inductive Coupled Plasma (ICP) in a Jovin Yvon instrument (JY-70 plus).

The particle morphology of the sample was studied by scanning electron microscopy (SEM) using a Jeol 6400 microscope.

Mössbauer spectroscopy was performed in a conventional spectrometer working at a constant acceleration mode with Co^{57} in a rhodium matrix as radioactive source. The spectra were analyzed using the NORMOS program (18).

Magnetization measurements were made at room temperature using an ASMI magnetometer (maximum magnetic field 14 kG with $\mathbf{H}d\mathbf{H}/dZ = 29\ kG^2cm^{-1}$).

Neutron diffraction measurements were performed at room temperature on the multi-detector powder diffractometer at the DR3 reactor at Risø National Laboratory. The sample was contained in a vanadium can of about 9 mm diameter and 50 mm length. Neutrons of wavelength 1.066(1) and 2.309(1) Å were chosen for these experiments The diffractometer was operated in the step scan mode with a step size of 0.05273° to measure 2000 profile points in all cases. The 2θ angular range was chosen in every case on the basis of the information to be obtained, thus for the short-wavelength experiment the diffraction pattern was collected betweeen 8° and 113.72° while this range was 20.0°–125.72° for the long-wavelength one. Diffraction data were analyzed using the program Fullprof (19). The scattering lengths for the different elements were $b(Fe) = 0.945 \times 10^{-12}$ cm, $b(Ni) = 1.030 \times 10^{-12}$ cm, and $b(O) = 0.5803 \times 10^{-12}$ cm. The magnetic form factors were calculated from Ref. (20).

RESULTS AND DISCUSSION

As deduced from chemical analysis the composition of the samples differs from that expected on the basis of an ideal exchange between sodium and nickel cations. Instead of getting a material of formula $NiFe_2O_4$, some iron is missing and some extra nickel is present. The final formulae for independent runs can be expressed as $Ni_{1+x}Fe_{2-2x/3}O_4$ with $0.25 \leq x \leq 0.35$. The results presented in this work correspond to a sample with $x = 0.3$; i.e., $Ni_{1.30}Fe_{1.80}O_4$.

Cubic spinels usually present cubic or octahedral morphology. In our case, as Figure 1 shows, a micaceous shape, reminiscent of the platelet-like morphology of the particles of the precursor α-$NaFeO_2$, is observed. This suggests the topotactic character of the ionic exchange reaction depicted in Eq. [1].

Crystal Structure

Preliminary structural characterization of the title material was performed by XRD. The pattern looks similar to that characteristic of the nickel ferrite prepared by the standard ceramic method (21). As already mentioned, X-ray powder diffraction is not the best technique to distinguish between iron and nickel atoms, neither to determine the oxygen stoichiometry; however, it is a preliminary source of information, thus, these data were analyzed by the Rietveld method. Some important results were obtained; in particular, a deficient occupation of the tetrahedral site, fully occupied in the ideal spinel structure and a partial occupation, about 10%, of the octahedral positions empty in the ideal spinel structure. The latter seems to be a consequence of the synthesis conditions and only appears if an excess of Ni(II) is used in the reaction. This suggests that these positions are mainly occupied by nickel ions.

In order to completely elucidate the complex cationic distribution suggested by the X-ray diffraction data, additional structural information was needed. Thus, neutron diffraction and Mössbauer spectroscopy measurements were performed.

Room temperature (RT) Mössbauer spectra (Fig. 2) can be used to determine the iron distribution between octahedral and tetrahedral available sites. About 57.3% of iron ions are located in tetrahedral sites, the rest being octahedrically coordinated. Taking into account these results, Ni ions should be mainly located in octahedral sites. The relevant hyperfine Mössbauer parameters are collected in Table 1.

Neutron powder diffraction data were used to refine both the nuclear and the magnetic structure of $Ni_{1+x}Fe_{2-2x/3}O_4$ ($x = 0.3$) at room temperature. To achieve the maximum resolution for the refinement of the nuclear structure,

FIG. 1. Scanning electron micrograph of the Ni–Fe spinel-like compound. The shape of the particles of the precursor α-$NaFeO_2$ is retained.

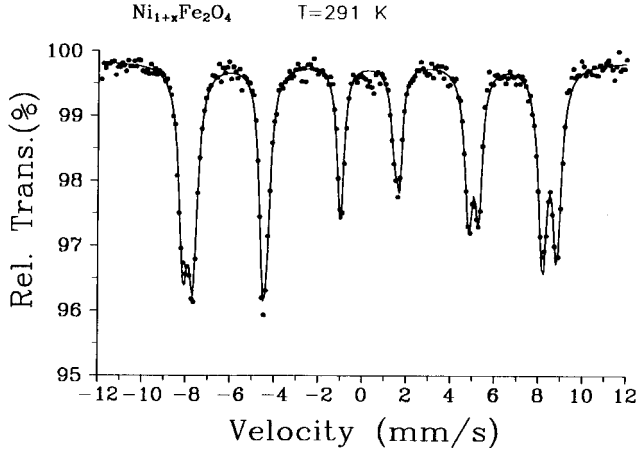

FIG. 2. Mössbauer spectrum at room temperature for the $Ni_{1+x}Fe_{2-y}O_4$ spinel-like compound.

neutrons of a short wavelength (1.066(1) Å) were chosen. Figure 3 shows the observed and calculated patterns and their difference. The refinement of our neutron diffraction data were made using the structural model that we proposed previously (14), taking into account the information

TABLE 1
Hyperfine Mössbauer Parameters for Nickel Ferrite at Room Temperature

	Octahedral positions	Tetrahedral Positions
H (KOe)	526	492
IS (mm/s)	0.36	0.25
ΔQ (mm/s)	− 0.01	0.19
Population Fe	42.7%	57.3%

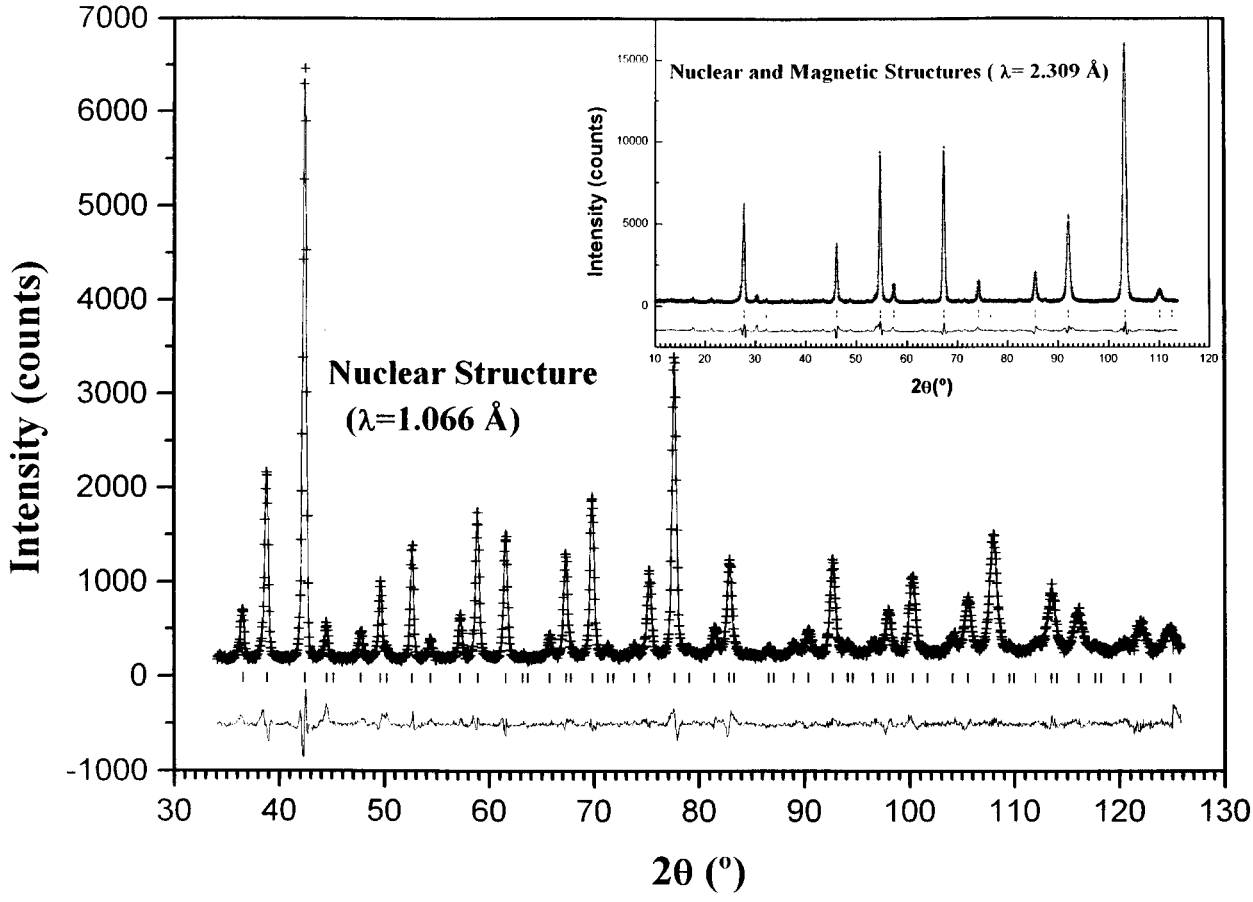

FIG. 3. Neutron diffraction patterns of $Ni_{1.25(1)}Fe_{1.85(1)}O_{4.00(1)}$ at room temperature. The solid line is the calculated (only nuclear structure) profile and the vertical marks correspond to the allowed Bragg reflections. The difference is plotted at the bottom of the figure. To minimize the magnetic component of the diffraction peaks neutrons of short wavelength ($\lambda = 1.066$ Å) were chosen and the low-angle region was excluded in the refinement. In the inset the experimental ($\lambda = 2.309$ Å) and calculated (nuclear and magnetic structures) profiles (and their difference) are shown. The first row and the second row of the vertical marks indicate the positions of the allowed peaks of the crystallographic and magnetic structures, respectively.

provided by chemical analysis, Mössbauer spectroscopy and X-ray diffraction data. The occupations of the 8*a*, 16*d*, and 16*c* sites as well as the oxygen stoichiometry were independently refined until convergence was reached. Table 2 collects the final structural parameters. These results are in good agreement with those obtained by other techniques; in particular, the partial occupation of the 16c sites by nickel ions observed by XRD was confirmed. In this connection, it is noticeable that for values of the *u* parameter greater than its ideal value 3/8, the 16*c* octahedral holes are larger than the 16*d* ones; the former being more suitable for accommodating divalent cations. On the other hand, the oxygen content was determined to be four atoms per unit formula; thus, the title compound can be considered as stoichiometric regarding the anion sublattice.

In a recent paper, Kesler *et al.* (15) studied the relationships between structures with occupied tetrahedra and octahedra in a cubic close packing of anions, in particular the series atacamite–spinel–halite (superstructure of NaCl). For doing so, these authors refer these structures to a spinel unit cell $a = a_{at} = a_{sp} = 2a_{NaCl}$ which contains 32 oxygen anions. The close packing of anions within this cell produces 32 octahedral holes (16*d* and 16*c* using the Wyckoff notation of the *Fd*3*m* space group) and 64 tetrahedral positions (8*a*, 8*b*, and 48*f*). In the atacamite structure only the 16*d* positions are occupied; while in the rock-salt one, both 16*d* and 16*c* octahedra host metal ions. On the other hand, in the spinel structure the octahedral 16*d* and the tetrahedral 8*a* sites are occupied. As Fig. 4 shows, the three structures have the atacamite framework B_2O_4 as a common feature. Worth to note, the octahedral 16*d* positions belonging to the atacamite framework have adjacent tetrahedral sites 8*b* and 48*f*, which are empty in the three structures. Thus, both types of holes (octahedral 16*d* and tetrahedral 8*b* and 48*f*) cannot be simultaneously occupied probably due to electrostatic repulsions. Some structures intermediate between

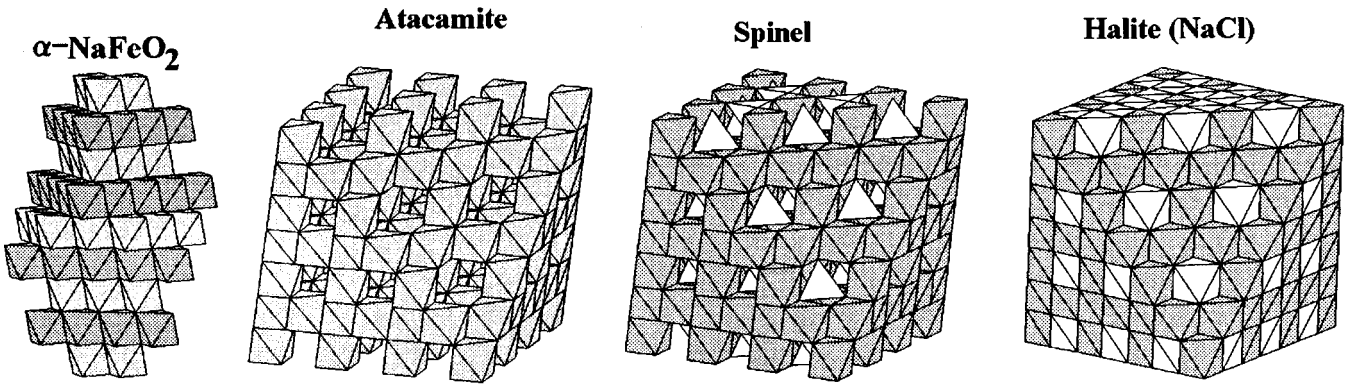

FIG. 4. Schematic representation of the structures of α-$NaFeO_2$, atacamite, spinel and halite (superstructure of NaCl). The atacamite framework can be thought of as being present in the four structures.

atacamite and spinel and between spinel and halite can be derived considering different ordered partial occupation schemes of nonatacamite sites (8*a* and 16*c*) within the atacamite framework Also, the atacamite framework B_2O_4 is present in both the precursor α-$NaFeO_2$ (B = Fe + Na) and in the nickel ferrite (B = Fe + Ni). In the spinel-like compound the 16*d* sites accommodate iron and nickel ions while in the precursor they are occupied by iron and sodium; the latter being removed by the ionic exchange reaction. Therefore, along the synthesis reaction this framework must be partially destroyed and reconstructed. This mechanism of reaction is different from that observed in other soft chemistry reactions like room temperature lithium insertion in Fe_3O_4 (22). In this case, using the ideas presented above, the formation of different phases as a function of the amount of lithium inserted can be understood in terms of topotaxy (15, 22).

Interestingly enough, Kesler *et al.* (15) predicted the existence of an ordered phase with partial occupation of both 8*a* (84.37%) and 16*c* (9.38%) sites, a cell parameter $a = 2a_{sp}$ and a $P\bar{4}3m$ symmetry. Although these site occupancies are similar to those of the title compound, we did not find evidence of additional ordering. This might be associated with the "reconstructive" nature of the present synthesis of the nickel ferrite. The oxygen sublattice of the precursor α-$NaFeO_2$ is retained in the synthesis reaction which can be thought to proceed through exchange and cationic redistribution into a close-packed network of oxygen (14). By exchange of monovalent Na(I) ions by divalent Ni(II) cations, half of the sodium sites in α-$NaFeO_2$ become vacant. In order to minimize the local electrostatic repulsions, a cationic redistribution takes place, giving rise to a complex site occupation scheme. Since Ni^{2+} cations, which are d^8 ions, show a clear tendency to occupy octahedral holes due to the crystal field stabilization, no nickel has been found in tetrahedral positions. Indeed, it must be recalled that the nickel ferrite obtained by the standard solid state reaction is an inverse spinel (1, 7). Other cations such as Mg(II) (which are d^0 ions with no crystal field stabilization) occupy both tetrahedral and octahedral holes (14).

Magnetic Structure

Magnetization curves for the title compound recorded at RT (Fig. 5) are typical of ferrimagnetic ordering with saturation magnetization $M(\mathrm{RT}) = 1.55\ \mu_B$/f.u. (37.05 emu/g). These values are in good agreement with those previously found (14). Assuming that the ratio of the saturation magnetization at room temperature to that at absolute zero (M_0) is 0.9 (23) the estimated value of M_0 is 1.72 μ_B; this value being quite different from that observed for standard $NiFe_2O_4$: $M_0 = 2.3\ \mu_B$/f.u. (56.0 emu/g) (1).

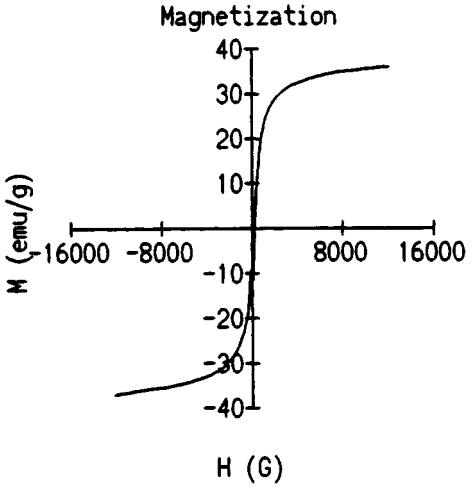

FIG. 5. Magnetization curve at room temperature for nickel–iron spinel-like material.

TABLE 2
Structure parameters of $Ni_{1+x}Fe_{2-y}O_4$

Atom	Site	x/a	y/b	z/c	Occup.	B_{iso} (Å)
Fe(1)	8*a*	0.0	0.0	0.0	0.99(1)	0.34(1)
Fe(2)	16*d*	5/8	5/8	5/8	0.86(1)	0.31(2)
Ni(1)	16*d*	5/8	5/8	5/8	1.14(1)	0.31(2)
Ni(2)	16*c*	1/8	1/8	1/8	0.11(1)	0.31(2)
O	32*e*	*u*	*u*	*u*	4.00(1)	0.74(4)

Note. $u = 0.38044(1)$, $a = 8.3353(2)$Å, S.G. *Fd3m*, Composition: $Ni_{1.25(1)}Fe_{1.85(1)}O_{4.00(1)}$; $R_B = 4.6\%$, $R_W = 8.2\%$, $R_p = 6.1\%$, $R_{exp} = 4.9\%$, $\chi^2 = 2.8$, $^{16d}|\mu|_{Fe} = 4.2(1)\ \mu_B$, $^{8a}|\mu|_{Fe} = 3.7(1)\ \mu_B$, $\langle|\mu|_{Ni}\rangle = 1.5(1)\ \mu_B$; $\phi = 33^\circ(1)$, $R_M = 4.47\%$.

The magnetic moment can be estimated taking into account the cationic distribution shown in Table 2 and assuming the following model for the magnetic structure: (a) the collinear ordering of ferrimagnetic spinels is maintained and (b) the magnetic moments of the extra ions in the 16*c* positions are antiparallel to those in 16*d* sites while they are parallel to the magnetic moments of ions in 8*a* sites. The latter hypothesis is supported by the geometrical information shown in Table 3. The superexchange interaction between two cations via an intermediate oxygen ion is the greatest whenever the three ions are collinear and their distances are not too large. Therefore, the angles and the distances between ^{8a}Fe(1) and ^{16d}M and between ^{16d}M and ^{16c}Ni(2) are favorable for superexchange, being the only strong interactions in the spinel-like ferrite. Thus, the following model for the magnetic structure is proposed:

$$[x\mathrm{Fe}_{8a}\uparrow][(2-y)\mathrm{Fe}_{16d}\downarrow][y\mathrm{Ni}_{16d}\downarrow][z\mathrm{Ni}_{16c}\uparrow]. \quad [2]$$

At this point it must be noticed that Mössbauer spectroscopy indicates that iron is only present in nickel ferrite as trivalent cation.

TABLE 3
Selected Geometrical Information: Distances < 2.5 Å and Angles (°)

^{8a}Fe(1)–O	$1.885(1)\times 4$
^{16d}M–O	$2.038(1)\times 6$
^{16c}Ni(2)–O	$2.131(1)\times 6$
^{8a}Fe(1)—O–^{16d}M	123.4(6)
^{8a}Fe(1)–O–^{16c}Ni(2)	53.4(6)
^{16d}M–O–^{16d}M	92.6(4)
^{16d}M–O–^{16c}Ni(2)	90(1)
^{16d}M–O–^{16c}Ni(2)′	176(1)
^{16c}Ni(2)–O–^{16c}Ni(2)′	87.4(6)

Thus, the net moment in Bohr magnetons can be expressed as

$$\mu(\mu_B) = x\mu_{Fe(III)} - (2-y)\mu_{Fe(III)} - y\mu_{Ni(II)} + z\mu_{Ni(II)}, \quad [3]$$

where $\mu_{Ni(II)} = 2\ \mu_B$, $\mu_{Fe(III)} = 5\ \mu_B$ (24) are the spin-only values of the magnetic moments of Ni^{2+} and Fe^{3+} cations.

The magnetic moment estimated by applying this model is 1.41 μ_B/f.u. As in the "standard" nickel ferrite, the difference between calculated and experimental values of M_0 (2.0 μ_B/f.u. and 2.3 μ_B/f.u respectively) arises from incomplete quenching of the orbital momentum of Ni^{2+} ions (1, 7). When this effect is corrected, the magnetization saturation at 0 K can be estimated as 1.72 μ_B in very good agreement with the experimental value. Since the saturation magnetization is very sensitive to the cationic distribution, the agreement between the experimental and the calculated values of M_0 strongly supports the site occupation scheme depicted in Table 2.

The neutron powder diffraction data shown in Fig. 3 indicate that, as observed in other ferrimagnetic spinels (1), the magnetic unit cell is identical to that of the nuclear structure. It is well known that in high symmetry magnetic structures the spin direction cannot be deduced from powder data (25). However, when the so-called configurational symmetry associated with the magnetic structure is tetragonal, rhombohedral or hexagonal, powder diffractograms can provide information about the angle between the spin direction and the unique axis of the structure. If the collinear ferrimagnetic structure represented by Eq. [2] is assumed, the configurational symmetry of the title compound belongs to the $R\bar{3}$ space group, the unique axis being the $[111]_c$ cubic direction.

In most of uniaxial structures, the spin lies in a direction parallel or perpendicular to the unique axis. However, a preliminary study of contribution of the magnetic scattering to the peaks, in particular to the (111) (at 27.8° in the inset of Fig. 3) and the (220) (at 46.2°) peaks, suggested that the angle between the magnetic moment and the unique axis is intermediate between 0° and 90°. In other ferrites, for instance Fe_3O_4, the magnetic moments lie in the $[100]_c$ direction (26), which forms an angle of 54.7° with the $[111]_c$ direction. Thus, we used as starting model for the magnetic structure that shown in Eq. [2] with the cationic distribution collected in Table 2 and the spin aligned along the cubic *a-axis*. Assuming this model, we refined the neutron powder diffraction data recorded using neutrons of a large wavelength ($\lambda = 2.309(1)$ Å) to maximize the magnetic contribution to the diffraction peaks (inset of Fig. 3). Some weak reflections are observed in the inset of Fig. 3 corresponding to small amounts of an unidentified impurity phase produced in the reaction of synthesis, also detected by XRD. Because of the low occupancy of the 16*c* sites, the refinements were undertaken with the restriction of making identical the absolute values of the three components of the

magnetic moments of Ni(II) in 16*c* and 16*d* positions. If the spins are constrained to lie in the *a*-axis, a value of 8.6% is reached for the magnetic structure agreement factor (R_M). If the magnetic moments are allowed to be out of the *a*-axis, the fitting is significantly improved; when convergence is reached the R_M factor is 4.5%. The angle between the spin direction and the unique axis $[111]_c$ is 33(1)° instead of 54.7°. The final parameters for the magnetic structure are collected in Table 2.

The value of the magnetic moment of iron in the 16*d* octahedral site is 4.2 μ_B, which is close to value corresponding to the free ion Fe^{3+} (5 μ_B); in contrast, the magnetic moment of iron in 8*a* positions (3.7 μ_B) is considerably lower than this value. This reduction can be explained by strong covalency effects due to the short Fe(1)–O distances (1.885 Å, see Table 3). In the case of nickel, the magnetic moment is 1.5(1) μ_B which is lower than that expected for Ni^{2+} (2 μ_B). It is worth noting that commonly nickel cations in octahedral coordination, as in La_2NiO_4 (27), show saturation moments similar to that determined in the title compound. This reduction is explained by covalency effects and quantum spin fluctuations (27). Using the magnetic moments collected in Table 2, a value of the saturation moment at room temperature of 1.5(1) μ_B is calculated, in good agreement with the experimental result 1.55 μ_B.

CONCLUDING REMARKS

To summarize the above results, we have confirmed by neutron diffraction, the existence of a nonstoichiometric phase intermediate between the rock-salt and the spinel types where some extra octahedral positions, occupied in the former but empty in the latter, are partially occupied.

On the other hand, the refined magnetic structure agrees with the collinear model proposed for most of the spinel-like compounds. The spins are somewhat deviated from the *a*-axis; the angle formed by the direction of the magnetic moments and the unique axis of the magnetic structure $[111]_c$ is $\phi = 33°(1)$.

ACKNOWLEDGMENTS

We thank CICYT (Project Mat 95-0809) and the EEC-LIP Program for financial support. We want to express our gratitude to Mr. F. Rojas (Dpt. Química Inorgánica, U.C.M.) for his help in the magnetization measurements and to Dr. N. Menéndez and Professor J. D. Tornero (Dpt. Química Física Aplicada, U.A.M.) for recording the Mössbauer spectra. We are also indebted to Professor M. A. Alario-Franco (Dpt. Química Inorgánica, U.C.M.) and Dr.J. L. Martínez (ICMM-CSIC) for carefully reading the manuscript and for valuable comments.

REFERENCES

1. J. Smit and H. P. J. Wijn, "Ferrites." Technical Library Philips, Eindhoven, The Netherlands, 1961.
2. J. Rivas, J. Iñiguez, and J. Ayala, *Appl. Phys.* **19,** 71 (1979).
3. L. Torres, M. Zazo, J. Iñiguez, C. de Francisco, and J. M. Muñoz, *IEEE Trans. Magnetics* **29,** 6 (1993).
4. B. Durand, J. M. Pàris, and M. Escoubes, *Ann. Chim. Fr.* **3,** 135 (1978).
5. J. Miki, M. Asanuma, Y. Tachibana, and T. Shikada, *J. Catal.* **151,** 323 (1995).
6. T. Kodama, Y. Wada, T. Yamamoto, M. Tsui, and Y. Tamaura, *Matter Res. Bull.* **30**(8), 1039 (1995).
7. J. M. Hastings and L. M. Corliss, *Rev. Mod. Phys.* **25**(1), 114 (1953).
8. L. Torres, M. Zazo, J. Iñiguez, C. de Francisco, and J. M. Muñoz, *J. Magn. Magn. Mater.* **140,** (1995).
9. R. H. Kodama, C. L Seaman, A. E. Berkowitz, and M. B. Maple, *J. Appl. Phys.* **75,** 10 (1994).
10. J. Beretka and T. Brown, *J. Am. Ceram. Soc.* **66,** 383 (1983).
11. R. E. Carter, *J. Am. Ceram. Soc.* **44,** 116 (1961).
12. J. A. Chatterjee, D. Das, S. K. Pradhan, and D. Chakravorty, *J. Magn. Magn. Mater.* **127,** 214 (1993).
13. W. A. England, J. B. Goodenough, and X. Wiseman, *J. Solid State Chem.* **49,** 289 (1983).
14. M. C. Blesa, U. Amador, E. Morán, N. Menéndez, J. D. Tornero, and J. Rodríguez-Carvajal, *Solid State Ionics* **63–65,** 429 (1993).
15. Y. A. Kesler and D. S. Filimonov, *Inorg. Mater.* **30**(11), 1255 (1994).
16. A. R. Landa-Cánovas and L. C. Otero-Díaz, *Solid State Ionics* **63–65,** 378 (1993).
17. Y. Takeda, *Mater. Res. Bull.* **15,** 1167 (1980).
18. R. A. Brand, *Nucl. Instrum. Methods Phys. Res. B* **28,** 398 (1987).
19. J. Rodríguez-Carvajal, Abstract of the Satellite Meeting of the XVth Congress of the International Union of Crystallography, Toulouse, France, 1990.
20. P. J. Brown, Institut Laue-Langevin Report SP88BR5016 (1988).
21. ASTM card 10-325, ASTM card 17-464
22. M. M. Thackeray, W. I. F. David, and J. B. Goodenough, *Mater. Res. Bull.*, **17,** 785 (1982).
23. R. Pauthenet and L. Bochirol, *J. Phys. Radium.* **12,** 249 (1951).
24. A. H. Morrish, "The Physical Principles of Magnetism," 5th ed., p. 507. Krieger, Malabar, FL 1983.
25. G. Shirane, *Acta Crystallogr.* **12,** 282 (1959).
26. W. C. Hamilton, *Phys. Rev.* **110**(5), 1050 (1958).
27. J. Rodríguez-Carvajal, M. T. Fernández-Díaz and J. L. Martínez, *J. Phys.: Condens. Matter.* **3,** 3215 (1991) and references therein.